The Meteoritical Society

Meteoritics & Planetary Science 49, Nr 9, 1509–1521 (2014)
doi: 10.1111/maps.12168

Stardust Interstellar Preliminary Examination I: Identification of tracks in aerogel

Andrew J. WESTPHAL[1*], David ANDERSON[1], Anna L. BUTTERWORTH[1], David R. FRANK[2], Robert LETTIERI[1], William MARCHANT[1], Joshua VON KORFF[1], Daniel ZEVIN[1], Augusto ARDIZZONE[3], Antonella CAMPANILE[4], Michael CAPRARO[5], Kevin COURTNEY[6], Mitchell N. CRISWELL III[7], Dixon CRUMPLER[8], Robert CWIK[9], Fred Jacob GRAY[10], Bruce HUDSON[11], Guy IMADA[12], Joel KARR[13], Lily Lau Wan WAH[14], Michele MAZZUCATO[15], Pier Giorgio MOTTA[15], Carlo RIGAMONTI[16], Ronald C. SPENCER[17], Stephens B. WOODROUGH[18], Irene Cimmino SANTONI[19], Gerry SPERRY[20], Jean-Noel TERRY[21], Naomi WORDSWORTH[22], Tom YAHNKE SR.[23], Carlton ALLEN[24], Asna ANSARI[25], Saša BAJT[26], Ron K. BASTIEN[2], Nabil BASSIM[27], Hans A. BECHTEL[28], Janet BORG[29], Frank E. BRENKER[30], John BRIDGES[31], Donald E. BROWNLEE[32], Mark BURCHELL[33], Manfred BURGHAMMER[34], Hitesh CHANGELA[35], Peter CLOETENS[34], Andrew M. DAVIS[36], Ryan DOLL[37], Christine FLOSS[37], George FLYNN[38], Zack GAINSFORTH[1], Eberhard GRÜN[39], Philipp R. HECK[40], Jon K. HILLIER[41], Peter HOPPE[42], Joachim HUTH[42], Brit HVIDE[25], Anton KEARSLEY[43], Ashley J. KING[44], Barry LAI[45], Jan LEITNER[42], Laurence LEMELLE[46], Hugues LEROUX[47], Ariel LEONARD[37], Larry R. NITTLER[48], Ryan OGLIORE[49], Wei Ja ONG[37], Frank POSTBERG[41], Mark C. PRICE[33], Scott A. SANDFORD[50], Juan-Angel Sans TRESSERAS[34], Sylvia SCHMITZ[30], Tom SCHOONJANS[51], Geert SILVERSMIT[51], Alexandre S. SIMIONOVICI[52], Vicente A. SOLÉ[34], Ralf SRAMA[53], Thomas STEPHAN[36], Veerle J. STERKEN[54], Julien STODOLNA[1], Rhonda M. STROUD[27], Steven SUTTON[45], Mario TRIELOFF[41], Peter TSOU[55], Akira TSUCHIYAMA[56], Tolek TYLISZCZAK[28], Bart VEKEMANS[51], Laszlo VINCZE[51], and Michael E. ZOLENSKY[24]

[1]Space Sciences Laboratory, U.C. Berkeley, Berkeley, California, USA
[2]ESCG, NASA JSC, Houston, Texas, USA
[3]Red Team, via Simone Cuccia, 45, Palermo, Italy
[4]Red Team, Reggio Emilia, Italy
[5]Red Team, 13998 Kingswood, Riverview, Michigan, USA
[6]Red Team, 918 Toni Marie Ct., Ballwin, Missouri, USA
[7]Red Team, Dog Star Observatory, P.O. Box 528, Pearce, Arizona, USA
[8]Red Team, Durham, North Carolina, USA
[9]Red Team, Rosewood Circle, Silver City, New Mexico, USA
[10]Red Team, Hampton, South Carolina, USA
[11]Red Team, Ontario, Canada
[12]Red Team, Brookings, Oregon, USA
[13]Red Team, 9812 N Lydia Ave, Kansas City, Missouri, USA
[14]Red Team, 93 Yishun St 81, Tower 8 #10-07, Orchid Park Condo, Singapore
[15]Red Team, Italy
[16]Red Team, Strada della Rovere 3/z, Moncalieri, Italy
[17]Red Team, Leominster, Massachusetts, USA
[18]Red Team, 100 Beach Drive, Suite 1801-03, St. Petersburg, Florida, USA
[19]Red Team, 40 Oak Drive, Upper Saddle River, New Jersey, USA
[20]Red Team, Tacoma, Washington, USA
[21]Red Team, Tarentaise, France
[22]Red Team, South Buckinghamshire, UK
[23]Red Team, 5231 Jamieson Ave 1-S., Louis, Missouri, USA
[24]ARES, NASA JSC, Houston, Texas, USA
[25]Robert A. Pritzker Center for Meteoritics and Polar Studies, The Field Museum of Natural History, Chicago, Illinois, USA
[26]DESY, Hamburg, Germany

[27]Materials Science and Technology Division, Naval Research Laboratory, Washington, District of Columbia, USA
[28]Advanced Light Source, Lawrence Berkeley Laboratory, Berkeley, California, USA
[29]IAS Orsay, Orsay, France
[30]Geoscience Institute, Goethe University Frankfurt, Frankfurt, Germany
[31]Space Research Centre, University of Leicester, Leicester, UK
[32]Department of Astronomy, University of Washington, Seattle, Washington, USA
[33]University of Kent, Canterbury, Kent, UK
[34]European Synchrotron Radiation Facility, Grenoble, France
[35]George Washington University
[36]University of Chicago, Chicago, Illinois, USA
[37]Washington University, St. Louis, Missouri, USA
[38]SUNY Plattsburgh, Plattsburgh, New York, USA
[39]Max-Planck-Institut für Kernphysik, Heidelberg, Germany
[40]Field Museum of Natural History, Chicago, Illinois, USA
[41]Institut für Geowissenschaften, University of Heidelberg, Heidelberg, Germany
[42]Max-Planck-Institut für Chemie, Mainz, Germany
[43]Natural History Museum, London, UK
[44]The University of Chicago and Robert A. Pritzker Center for Meteoritics and Polar Studies,
The Field Museum of Natural History, Chicago, Illinois, USA
[45]Advanced Photon Source, Argonne National Laboratory, Chicago, Illinois, USA
[46]Ecole Normale Superieure de Lyon, Lyon, France
[47]University Lille 1, France
[48]Carnegie Institution of Washington, Washington, District of Columbia, USA
[49]University of Hawai'i at Manoa, Honolulu, Hawai'i, USA
[50]NASA Ames Research Center, Moffett Field, California, USA
[51]University of Ghent, Ghent, Belgium
[52]Institut des Sciences de la Terre, Observatoire des Sciences de l'Univers de Grenoble, Grenoble, France
[53]IRS, University Stuttgart, Stuttgart, Germany
[54]IRS, University Stuttgart, Stuttgart, IGEP, TU Braunschweig, Braunschweig, Germany and MPIK, Heidelberg, Germany
[55]Jet Propulsion Laboratory, Pasadena, California, USA
[56]Osaka University, Osaka, Japan
*Corresponding author. E-mail: westphal@ssl.berkeley.edu

(Received 05 December 2012; revision accepted 14 June 2013)

Abstract–Here, we report the identification of 69 tracks in approximately 250 cm^2 of aerogel collectors of the Stardust Interstellar Dust Collector. We identified these tracks through Stardust@home, a distributed internet-based virtual microscope and search engine, in which > 30,000 amateur scientists collectively performed $>9 \times 10^7$ searches on approximately 10^6 fields of view. Using calibration images, we measured individual detection efficiency, and found that the individual detection efficiency for tracks > 2.5 μm in diameter was >0.6, and was >0.75 for tracks >3 μm in diameter. Because most fields of view were searched >30 times, these results could be combined to yield a theoretical detection efficiency near unity. The initial expectation was that interstellar dust would be captured at very high speed. The actual tracks discovered in the Stardust collector, however, were due to low-speed impacts, and were morphologically strongly distinct from the calibration images. As a result, the detection efficiency of these tracks was lower than detection efficiency of calibrations presented in training, testing, and ongoing calibration. Nevertheless, as calibration images based on low-speed impacts were added later in the project, detection efficiencies for low-speed tracks rose dramatically. We conclude that a massively distributed, calibrated search, with amateur collaborators, is an effective approach to the challenging problem of identification of tracks of hypervelocity projectiles captured in aerogel.

INTRODUCTION

The primary mission of the NASA Discovery-class mission Stardust was to return a sample of cometary material from the coma of Jupiter-family comet 81P/Wild 2 (Tsou et al. 2003). But Stardust was effectively two missions in one spacecraft—the second mission was to return a sample of contemporary interstellar dust, and, to that end, the spacecraft carried a tray of aerogel and aluminum foil that was exposed to the interstellar dust stream during two periods before the encounter with the comet. After the successful recovery of the collector in 2006, NASA initiated a preliminary examination (PE) of the Stardust interstellar collector. This was the fourth PE that NASA has conducted on returned extraterrestrial samples, after Apollo, Genesis, and the Stardust cometary dust collection.

The first order of business, before any interstellar dust candidates could be extracted from the collector and analyzed, was simply to identify them. The challenge is straightforward: to identify tracks of approximately 1 μm particles, it was necessary to search at sufficiently high magnification ($\leq$0.5 μm pixel^{-1}) in an optical microscope. A simple estimate quickly showed that of order one million fields of view would have to be searched. Before launch, Landgraf et al. (1999) predicted that approximately 50 interstellar dust particles would be captured in the collector, so only one field of view in approximately 20,000 would contain a track. A search of this magnitude was beyond the capability of any professional research group. This collaboration, therefore, includes more than 30,000 amateur scientists. "Citizen Science" is enjoying a new vogue with the advent of the internet, but, in fact, there is a long tradition of highly productive participation of amateurs in astronomy. This approach has some parallels with Operation Moonwatch at the dawn of the space age (McCray 2008). So far, we have identified 69 tracks in the aerogel collectors, including 22 that appear to be consistent in their trajectories with an origin in the interstellar dust stream (Frank et al. 2013; Sterken et al. 2014) or as secondaries from impacts on the Sample Return Capsule, which was in the field of view of the collector.

METHODS

The Stardust Mission

The Stardust spacecraft was launched on 7 Feb 1999 21:31 UTC. The interstellar collector was exposed for two periods to the interstellar dust stream: from 22 Feb 2000 to 1 May 2000 and from 5 Aug 2002 to 9 Dec 2002 (Tsou et al. 2003). The heliocentric distance of the spacecraft was 2.1–2.2 AU during the first exposure, and 2.2–2.6 AU for the second exposure. The total exposure time was 195 days. The collector tracked the interstellar dust stream such that particles with $\beta = 1$ would have been captured at normal incidence. Here, β is the dimensionless ratio of the force due to radiation pressure from sunlight to the gravitational force. The interstellar dust stream was assumed to originate from ecliptic latitude +8° ecliptic longitude +259°. The spacecraft attitude was maintained in a deadband of ±15° in all three axes during the exposures, with brief excursions for communication and navigation.

Stardust Interstellar Dust Collector

The Stardust interstellar collector comprised 132 aerogel tiles, approximately 283 aluminum foils, and the aluminum collector frame itself. One hundred thirty aerogel tiles presented a rectangular face measuring 20 × 40 mm to space, and two tiles were polygonal in shape and somewhat smaller in area. All interstellar tiles were 10 mm thick, and had an average density of approximately 26 mg cm^{-3} (Butterworth et al. 2014). The total area of the aerogel portion of the collector was approximately 1039 cm^2.

Image Data Collection

We used an automated microscope to collect digital imagery of aerogel tiles in the Stardust Interstellar Collector. All scanning was carried out in the Cosmic Dust Laboratory at the Johnson Space Center in Houston. We used a customized Leica Metalloplan microscope with an automated stage (Technical Instruments) controlled by computer (Apple Mac Mini) through a stage controller (Compumotor 6K4). The stage positioning accuracy was <2 μm. We used a 1024 × 768 monochromatic CCD camera (Flea, Point Grey Research) mounted on the camera port of the microscope, and a 10× objective. Image data were collected at 15 Hz, using the Astro IIDC image acquisition package (Outcast Software) running on a desktop computer (Apple Mac Mini). The field of view was 480 × 360 μm, so the spatial resolution, as defined by the size of a pixel projected onto the tray, was 0.47 μm pixel^{-1}. This is comparable to the intrinsic diffraction limit of the microscope.

We scanned one tile at a time. We wrote programs in MATLAB to generate Unix scripts for making semiautomated altitude maps of each aerogel tile and for fully automated scanning. First, we used a semiautomated script and manual focusing to measure

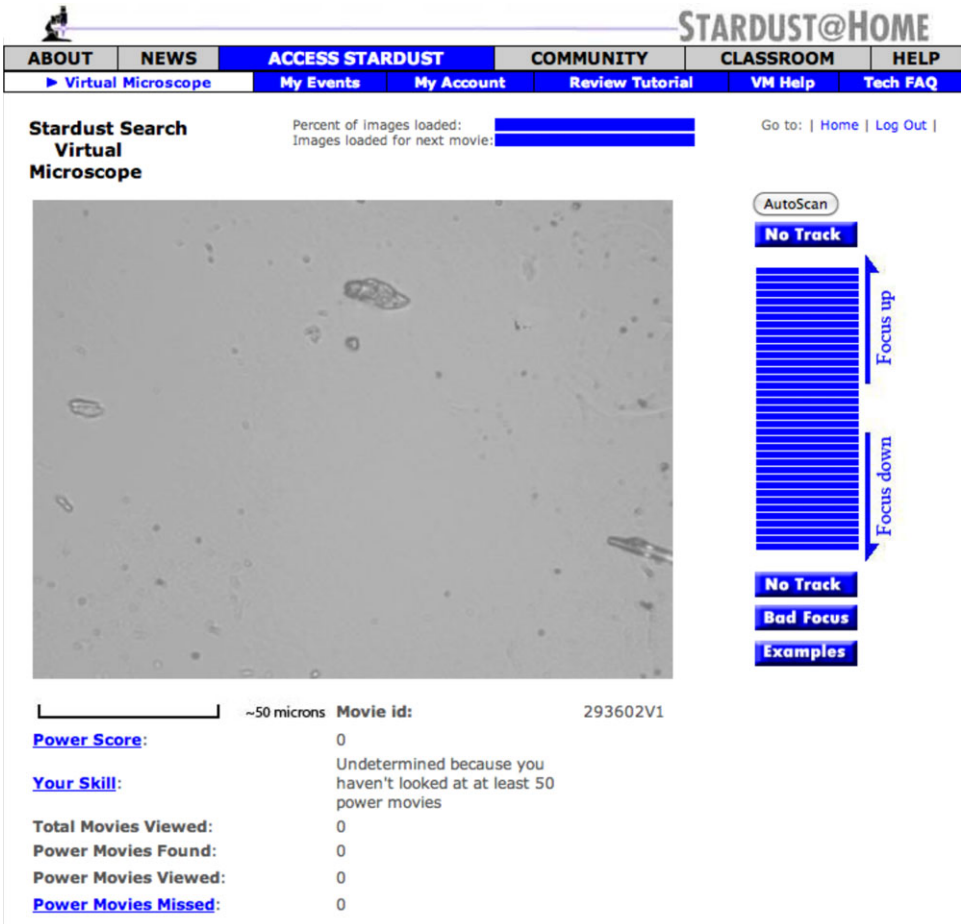

Fig. 1. A screen shot of the Stardust@home virtual microscope.

the height of the aerogel tile over a 10 × 20 grid. This step was required because the aerogel tiles exhibit smooth, but large-amplitude, topography. We then used this altitude map to generate a script for fully automated scanning, and used a spline interpolation between measured altitudes to define the surface altitude for each field of view. The outer 1–2 mm of each tile was typically heavily fractured, so these areas were not scanned.

In each field of view, the scanning system collected a QuickTime stack, called a "focus stack," consisting of approximately 50 frames acquired during a slow slew of the microscope's vertical axis through approximately 200 μm. The scan started approximately 50 μm above the interpolated aerogel surface and ended approximately 150 μm below the interpolated surface. Because of slight variations in the timing of the beginning of recording the focus stack, these positions varied by several micrometers. Each stack was stored on an external disk, with a filename that included the coordinates of the stack; 200–300 Mb of data storage was required for each tile. We collected approximately 250,000 focus stacks.

Stardust@Home Distributed Search

We searched for candidate interstellar dust impacts in the image data using a massively distributed, internet-based search tool that we called Stardust@home (S@H). Two of us, Dave Anderson and Josh Von Korff, designed and wrote a virtual microscope (VM) that ran natively in html and Java on common internet-connected Web browsers. In Fig. 1, we show the Stardust@home Virtual Microscope as it appeared to volunteers.

We prepared the raw focus stacks for internet-based searching by splitting them into individual frames, and compressing each frame in compressed jpeg format. We did this processing automatically using Applescript and the image processing capability of QuickTime Professional. After this processing, we uploaded the image data to the Amazon S3 "cloud." These images

were then available for downloading to the VM as described below.

Through one of the online forums on the Stardust@home website, those of us among the Stardust@home volunteers named ourselves "dusters." We adopt the same nomenclature here. To qualify to become a duster, a volunteer was required first to go through a training session on the Stardust@home website, and, after training, to pass an online test with at least eight correct responses to ten test images. After passing this qualification test, we were invited to register as Stardust@home dusters. As of 23 Jan 2012, 30,649 people passed the test and registered as S@H dusters.

We searched image data as follows. The client browser initiated the search by sending a request to the S@H server for a VM webpage. The VM generated a new webpage automatically by choosing a focus stack randomly from a list of available focus stacks. Approximately 43 frames of image data were loaded onto the client browser, but only one was displayed at a time. We slewed through the stack of images by moving the computer cursor along a focus bar located adjacent to the image window. By moving the cursor, we focused up and down through the stack of images, thus simulating what one would see if turning the focus knob on a real microscope and looking at the same field of view.

We then responded to the focus stack in one of three ways. If no candidate track was identified, we pressed a "no track" button, and this response was recorded in the database by the server, along with supporting information (volunteer identification, stack identification, and time). If a candidate was found, we clicked on the location of the deepest feature in the candidate track that was visible in the focus stack. We then were asked to confirm the identification before the positive response and the coordinates of the click were recorded in the database, along with supporting information, such as a timestamp. Finally, if no surface could be identified, or if the topography within the field of view prevented an adequate search, we responded by clicking a "bad focus" button. This response was also be recorded by the server along with supporting information. In all cases, the VM running on the client browser would then automatically request and serve up the next focus stack for searching.

We measured detection efficiencies and rate of false positives (the equivalent of noise rate in an electronic detector) using images with known characteristics—so-called calibration stacks. Half of the calibration stacks were focus stacks from the general data set into which the image of a 12 μm diameter track was dubbed. The track image was randomly rotated through 2π and scaled in diameter and independently in depth. The scale factor in diameter was chosen randomly in the range 0.2–2.0. The other half of the calibration stacks were focus stacks from the Stardust Interstellar data set, which we had carefully examined and determined to be blank. The types and numbers of calibration focus scans were varied through the various phases of the S@H project (see the next section). Any given search had a 20% probability of being a calibration stack. During scanning on the VM, we knew in general that some stacks were calibration stacks, but the VM presented no information that would allow us to know whether any specific stack was a calibration stack or not.

The use of calibration stacks had two serendipitous advantages. First, we used the responses to calibration stacks to automatically generate an individual, real-time score for each of us. The score simply consisted of the number of correct responses to calibration stacks less the number of incorrect responses. Although we did not use this score in any data analysis, we found that maintaining a score was highly motivating for many of us. Second, we found that the frequent presentation of calibrations helped to maintain attention. Attention is difficult to maintain in lengthy searches for rare events.

Stardust@Home Phases

Phase I

Phase I was the initial phase of Stardust@home. Calibrations were of two types: known blanks, which we had searched for candidate tracks, and positive stacks, in which the image of a single track was digitally dubbed. The track was rotated randomly through 2π and scaled in size both in depth and in projection, between 0.2 and 2.0 in magnification.

Phase II

Here, we processed and presented "high-res" stacks. Because stacks were compressed for uploading to Stardust@home, the compression resulted in some degradation of image quality. We therefore reprocessed the raw image data by dividing each field of view into quarters and recompressing them. We uploaded these "high-res" images to Stardust@home. These images were presented with a corrected scalebar on the Stardust@home viewer.

Phase III

In Phase III, we added new calibration stacks, based on the image of "whisker-like" feature in the Stardust aerogel, and upgraded the training and testing procedure to include this. We re-examined all stacks during Phase III.

Table 1. Statistics of each phase of Stardust@home.

Phase	Launch date	End date	New dusters	Calibration stacks used	Total searched	Calibrations searched	Searches per duster
I	28 Jul 2006	30 Jul 2007	24176	2421	46.7×10^6	11.7×10^6	35
II	07 Aug 2007	09 Mar 2010	4396	3021	25.2×10^6	4.2×10^6	40
III	10 Mar 2010	04 Jul 2011	1683	1879	15.6×10^6	2.2×10^6	48
IV	12 Jul 2011	16 Jan 2011	458	17580	1.8×10^6	0.2×10^6	101
All phases	28 Jul 2006	>23 Jan 2012	30714		89.4×10^6	17.3×10^6	38

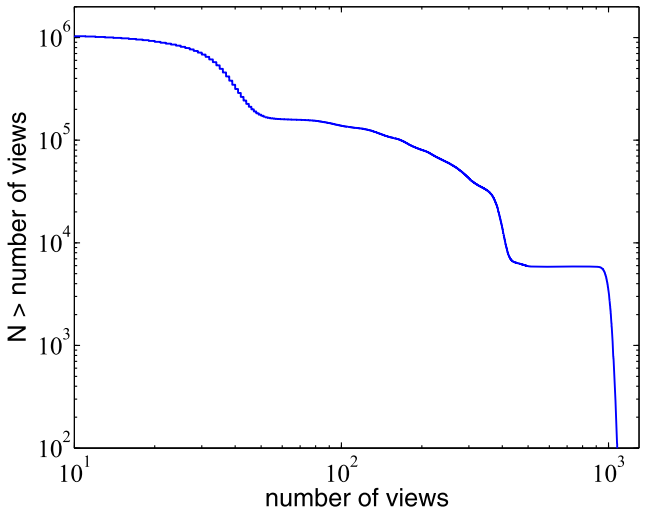

Fig. 2. Integral distribution of search statistics for focus stacks. The abscissa is the number of times that a stack was searched, and the ordinate is the number of stacks, which were searched at least that number of times. The steps in the statistics are due to large additions of image data to the database at discrete times.

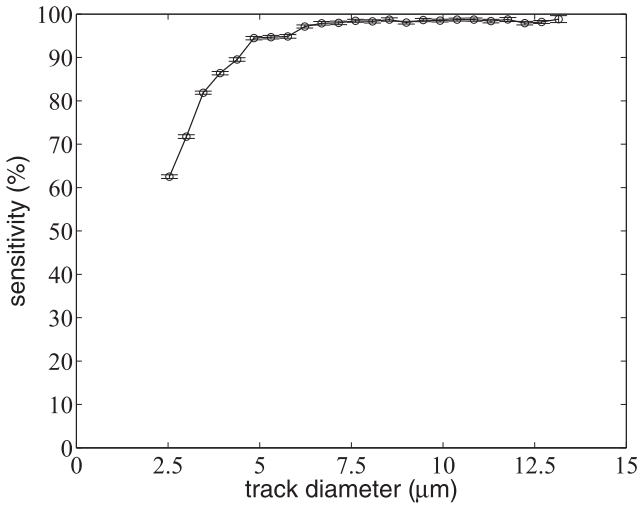

Fig. 3. Detection efficiency for calibration stacks during S@H Phases I (upper curve) and II (lower curve), based on 15.6×10^6 responses.

Phase IV

In Phase IV, we entirely replaced the calibration stack set with three different types of calibrations. The first type was similar to the calibrations in Phase I, but included both analog tracks and real tracks identified in the Stardust@home collector. The second type consisted of real, undubbed stacks in which tracks had been identified, but in four different configurations: as collected, rotated 180°, mirrored around the vertical axis, and mirrored around the vertical axis and rotated 180°. Finally, we included undubbed stacks of analog tracks, processed the same way. We re-examined all stacks during Phase IV.

Stardust@Home Statistics

In Table 1, we show the statistics for each Stardust@home phase.

In Fig. 2, we show the distribution of search statistics for each focus stack, as of 23 January 2012.

Calibration data from Phases I and II (Fig. 3) indicate an ensemble-wide average individual detection efficiency of ≥60% for hypervelocity tracks with diameter >2.5 μm, and ≥90% for hypervelocity tracks with diameter >5 μm. We emphasize that the *individual* detection efficiency is different from the *overall* detection efficiency, because of the large multiplicity of individual searches.

α-List

To efficiently identify candidate tracks, we employed two levels of selection. An intermediate list called the α-list consisted of preliminary candidates, and a final list of confirmed, unambiguous tracks was called the β-list. Candidates were selected for the α-list and β-list as follows.

For each field of view, we define ξ as the ratio of the number of positive identifications to the total number of searches conducted on that field of view. Periodically, we selected approximately 1000 stacks with the largest fraction ξ of positive responses from dusters to be promoted to the α-list, which corresponded to a promotion threshold value of $\xi = 0.2$ or smaller. By comparison, Phase I and II calibration data from high-velocity tracks show a detection efficiency of ≥0.75 for

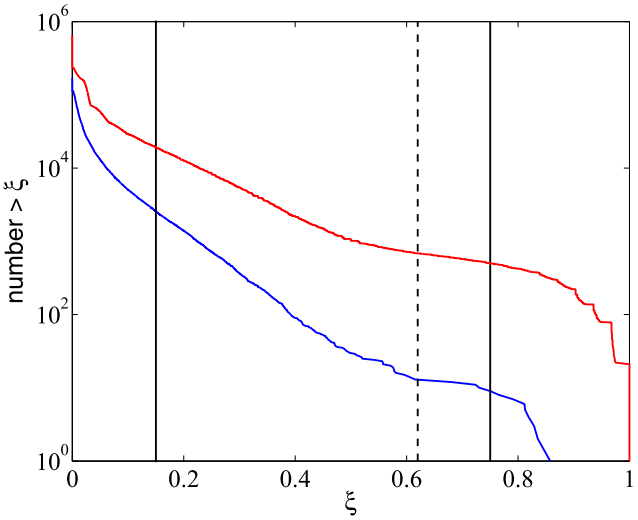

Fig. 4. Integral distribution of ξ for all stacks in phases I–IV. Red line: Stacks that were searched at least 30 times. Blue line: Stacks that were searched at least 50 times. The vertical line at $\xi = 0.75$ corresponds to the measured detection efficiency of tracks with diameter 3.0 μm, and the vertical line at $\xi = 0.62$ corresponds to this threshold adjusted for finite statistics with an average search multiplicity of 50. In practice, we examined all tracks with a cut far lower than this, with $\xi > 0.15$.

tracks >3 μm in diameter, so this threshold is highly conservative. In Fig. 4, we show the integral distributions of ξ for all stacks in phases I through IV, which had been searched ≥50 times, and ≥30 times. The effective search areas for these data sets are 225 cm^2 and 246 cm^2, respectively. Because, for any given field of view, the statistics are relatively small, statistical fluctuations in the number of positive identifications are expected. To compensate, one must lower the threshold to be sure to catch all of the positive detections. To illustrate, we imagine a data set consisting of stacks that have been searched 50 times, with a uniform detection efficiency of 0.75. Then, each stack would have collected, on average, 37.5 positive identifications. However, the distribution of positive identifications is approximately gaussian with a width of $\sqrt{37.5} \sim 6.1$, so, to be sure to identify 84% (1σ) of the actual tracks, one would set the threshold at $(37.5 - 6.1)/50 = 0.62$ For high-statistics stacks, those searched at least 50 times, 12 stacks fit this criterion. In practice, and to be highly conservative, at the end of phase IV, we individually reviewed all stacks with $\xi \geq 0.15$, 2256 focus stacks. For stacks that had been searched 30 times or more, we selected those with $\xi > 0.38$, which corresponds to 2473 stacks.

During Phase II, we invited the top-scoring dusters to join a so-called Red Team. The Red Team members, who were the most experienced dusters in the project, were given the system privileges to be able to promote any candidates, whom they thought interesting, into the α-list. The α-list, therefore, included three sets of candidates: those with $\xi > 0.15$ and $N_{search} > 50$, those with $\xi > 0.38$ and $N_{search} > 50$, and those who were promoted by the Red Team. The Red Team members were also able to rate, on a scale from 1 to 10, any of the stacks on the α-list.

One of us (AJW) reviewed all entries on the α-list, to identify *bona fide* tracks and candidate features that had the potential to be impacts, but were ambiguous. In this way, 69 tracks have now been identified, and included in the β-list of confirmed tracks. There are an additional 14 features that are ambiguous to varying extents, and may require extraction for definitive identification.

RESULTS

In Table 2, we show the list of candidate tracks that have been evaluated by the Berkeley group and confirmed as unambiguous tracks.

DISCUSSION

While the measured sensitivity for dust detection of calibrations was >0.62 over the range of calibration track diameters (>2.5 μm, Fig. 2), the measured efficiency for detection of actual tracks was generally considerably lower (Table 2). Almost all tracks found by Stardust@home had sizes near the detection threshold (approximately 2 μm), and differed strongly in appearance from the dubbed images in the original calibration stacks. The track image that was used in Phases I and II was due to a >15 km s^{-1} track generated by the Heidelberg Dust Accelerator (HDA) before the Stardust launch, so it was bulbous in appearance, in accordance with our initial expectations of the interstellar dust capture speed. But the tracks identified in the actual collector were morphologically similar to particles captured at low speed (≪ 10 km s^{-1}) observed in Heidelberg experiments (Postberg et al. 2014), and thus exhibited very small track diameter/length ratios (discussed further in Frank et al. [2013]). In Phase III, we included a very small linear feature in the calibration stacks, but this was different in appearance from the *bona fide* tracks. (The linear feature was later analyzed by synchrotron and determined to be a submicron fiber.) However, in Phase IV, we used calibration stacks of three types: stacks dubbed with randomly rotated and magnified images of previously identified *bona fide* tracks; actual stacks that include *bona fide* tracks, that we presented with four possible orientations (unchanged, reflection

Table 2. List of 69 tracks identified by the Stardust@home project. The columns are: stack number; azimuth angle of the particle trajectory in degrees, measured counterclockwise from the midnight (sunward) direction; the detection efficiency ξ and the number of searches for each of phases I through IV; the cumulative detection efficiency ξ and the number of searches; the first Stardust@home duster to identify the track; the Stardust@home Red Team members who identified and promoted the track to the α-list.

ID	ϕ	N_{I}	ξ_{I}	N_{II}	ξ_{II}	N_{III}	ξ_{III}	N_{IV}	ξ_{IV}	N_{mtotal}	ξ_{mtotal}	Duster discoverer	Red Team promoter(s)
225116V1	52	216	0.13	0	–	7	0.14	6	1	229	0.16	H Leithead	Fred J. Gray
237326V1	49	464	0.25	60	0.22	9	0.22	0	–	533	0.25	Pete Clearwater	Fred J. Gray
6065723V1													Jacopo Falchi Picchinesi
6544999V1													
305392V1	96	453	0.22	105	0.57	27	0.37	8	1	593	0.3	Ajay Chopra	SSL
2574341V1													Fred J. Gray
5406521V1													
8823383V1													
433711V1	47	482	0.21	1773	0.02	1029	0.01	0	–	3284	0.05	Michael Kopkow	SSL
7270647V1													
6634692V1													
451142V1	53	160	0.22	35	0.37	6	0.33	10	0.6	211	0.27	Devon Trevor Pollard	Augusto Ardizzone
8505527V1													
730481V1	42	473	0.19	2	0	28	0.54	0	–	503	0.21	Vance Thompson	Fred J. Gray
4065507V1													Lily Lau Wan Wah
862370V1	350	494	0.28	3	0	17	0.41	0	–	514	0.28	Stephan Wagner	Augusto Ardizzone
4009893V1													
1203103V1	351	305	0.04	33	0.06	12	0.17	0	–	350	0.05	Naomi Wordsworth	Fred J. Gray
2625717V1													Antonella Campanile
1303955V1	355	503	0.04	0	–	0	–	10	0.8	513	0.05	Bruce A Hudson	Fred J. Gray
3964782V1													
1728279V1	86	694	0.22	52	0.46	21	0.24	0	–	767	0.24	Elizabeth Wiggins	Mitchell Criswell
4566810V1													Fred J. Gray
6406644V1													
285812V1													
2205922V1	339	796	0.07	89	0.13	13	0.31	5	1	903	0.08	Robert Coursey	Fred J. Gray
2220548V1													Antonella Campanile
3303601V1													Gerry L. Sperry
5802607V1													
9276534V1													
3059039V1	58	859	0.16	125	0.07	30	0.07	0	–	1014	0.14	Jim Hinkey	Fred J. Gray
8153179V1													
2965266V1													
5202109V1													
5492352V1													
9040053V1													
3914098V1	358	124	0.04	25	0.04	10	0.3	6	0.67	165	0.08	Auggie Nanz	Fred J. Gray
3721744V1													Augusto Ardizzone

Table 2. *Continued.* List of 69 tracks identified by the Stardust@home project. The columns are: stack number; azimuth angle of the particle trajectory in degrees, measured counterclockwise from the midnight (sunward) direction; the detection efficiency ξ and the number of searches for each of phases I through IV; the cumulative detection efficiency ξ and the number of searches; the first Stardust@home duster to identify the track; the Stardust@home Red Team members who identified and promoted the track to the α-list.

ID	ϕ	N_{I}	ξ_{I}	N_{II}	ξ_{II}	N_{III}	ξ_{III}	N_{IV}	ξ_{IV}	N_{mtotal}	ξ_{mtotal}	Duster discoverer	Red Team promoter(s)
6355541V1 4720866V1 5159391V1 6150862V1	58	984	0.16	5	0	64	0.23	0	–	1053	0.17	Michael Hershberg	Lily Lau Wan Wah Michael A. Capraro
7387315V1 2717134V1 6839286V1	48	0	–	77	0.3	21	0.43	0	–	98	–	Gerald Bell	Michael A. Capraro
7703161V1 8130472V1	61	399	0.28	36	0.56	17	0.59	0	–	452	0.31	John Rote	SSL
8894764V1	356	182	0.11	0	–	4	0.75	3	1	189	0.14	Robert Kurt Myers	Joe Karr
9982449V1 3997562V1	30	472	0.21	5	0.4	26	0.35	0	–	503	0.22	Barry Weeg	SSL
9987464V1	48	257	0.09	0	–	0	–	4	0.75	261	0.1	Bruce A Hudson	Fred J. Gray
1779983V1 6133043V1	35	383	0.06	2	1	17	0.41	0	–	402	0.08	Paul M. Campbell	Michael A. Capraro
6389213V1	302	318	0.07	0	–	0	–	0	–	318	0.07	Pamela J. Copple	SSL
6721021V1 9925512V1	29	514	0.26	4	0.5	20	0.15	0	–	538	0.26	Fred Bruenjes	SSL Will Marchant
6842109V1 8729246V1	60	369	0.07	0	–	21	0.38	0	–	390	0.08	David Moses	SSL
7559378V1	56	299	0.06	0	–	0	–	5	0.8	304	0.07	Mieke Abels	SSL
7663035V1	3	263	0.02	0	–	0	–	6	0.83	269	0.04	Bruce A Hudson	Fred J. Gray
7933874V1	44	423	0.03	0	–	0	–	0	–	423	0.03	Dipali Vasadia	SSL
5103315V1	302	299	0.04	0	–	0	–	0	–	299	0.04	John Lokken	SSL
1078907V1	66	0	–	2	0	24	0.21	0	–	26	–	Patryk Kleman	Lily Lau Wan Wah
2344842V1 2595293V1 5256120V1	57	345	0.15	31	0.58	16	0.56	12	1	404	0.22	Daniel Lichtenwald	Mitchell Criswell Carlo Rigamonti Lily Lau Wan Wah
3160814V1	356	0	–	0	–	18	0.11	3	0	21	–	Patrick Fougeray	SSL
4359211V1	14	0	–	0	–	13	0.54	1	1	14	–	Kevin A Courtney	SSL
4969429V1	51	0	–	19	0.37	16	0.19	0	–	35	–	Michael A. Capraro	Michael A. Capraro
5848045V1 3689408V1	3	0	–	26	0.23	13	0.31	4	0.75	43	–	Steven E. Miles	Lily Lau Wan Wah Daniel Zevin
6125350V1 7810698V1	7	483	0.18	5	0	23	0.26	0	–	511	0.18	Gerald Fisher	SSL
6366986V1	51	0	–	33	0.42	5	0.6	0	–	38	–	Robert L Cwik	Mitchell Criswell
6474626V1	352	0	–	2	0	15	0.13	0	–	17	–	Augusto Ardizzone	SSL

Table 2. *Continued.* List of 69 tracks identified by the Stardust@home project. The columns are: stack number; azimuth angle of the particle trajectory in degrees, measured counterclockwise from the midnight (sunward) direction; the detection efficiency ξ and the number of searches for each of phases I through IV; the cumulative detection efficiency ξ and the number of searches; the first Stardust@home duster to identify the track; the Stardust@home Red Team members who identified and promoted the track to the α-list.

ID	ϕ	N_{I}	ξ_{I}	N_{II}	ξ_{II}	N_{III}	ξ_{III}	N_{IV}	ξ_{IV}	N_{mtotal}	ξ_{mtotal}	Duster discoverer	Red Team promoter(s)
6522857V1	44	129	0.13	30	0.27	11	0.36	3	0.67	173	0.18	Michael Paperin	SSL
2933051V1													
5088094V1	58	392	0.1	5	0.2	27	0.15	0	–	424	0.1	Mike Bunch	Mitchell Criswell
1306378V1													Michael A. Capraro
6535376V1	57	0	–	29	0.07	5	0	0	–	34	–	Michael A. Capraro	Michael A. Capraro
5599106V1	358	0	–	1	0	17	0.06	0	–	18	–	Joseph Moschetti	Fred J. Gray
1218276V1	26	0	–	0	–	5	0.4	6	0.33	11	–	Augusto Ardizzone	Augusto Ardizzone
5300933V1	55	145	0	0	–	8	0.75	4	0.75	157	0.06	Gerry L. Sperry	Michael A. Capraro
2599361V1	0	0	–	64	0.02	16	0.31	0	–	80	–	Ilya Alexeev	Augusto Ardizzone
3365250V1													
5484077V1	9	0	–	31	0.03	7	0.14	0	–	38	–	Charles Tabor	Michael A. Capraro
8250577V1	315	0	–	0	–	6		7	1	13	–	Gerry L. Sperry	Augusto Ardizzone
							0.5						
5198758V1	55	0	–	0	–	1038		0	–	1038	–	Tom Yahnke Sr.	Michael A. Capraro
							0.36						
9219038V1	55	0	–	0	–	984		0	–	984	–	Augusto Ardizzone	Augusto Ardizzone
							0.6						
661377V1	10	0	–	0	–	0		8	0.38	8	–	Michael A. Capraro	Michael A. Capraro
							–						
1506030V1	0	0	–	0	–	0		8	0.63	8	–	Martin St-pierre	Michael A. Capraro
							–						
2923270V1	73	82	0.17	0	–	7		7	0.29	96	0.17	Koorosh Mofazzali	SSL
							0						
4563629V1	351	0	–	0	–	0		5	1	5	–	Antonella Campanile	Antonella Campanile
							–						
6279005V1	335	179	0	0	–	6		6	0.33	191	0.01	Antonella Campanile	Antonella Campanile
							0						
8454485V1	27	0	–	0	–	0		7	0.57	7	–	Michael A. Capraro	Michael A. Capraro
							–						
8806280V1	50	0	–	0	–	7		6	1	13	–	Richard Koschier	Daniel Zevin
							0.29						
31269V1	72	0	–	0	–	0		6	0.67	6	–	Ivan Dimov	Carlo Rigamonti
							–						
9732478V1	158	0	–	0	–	0		6	0.83	6	–	Carlo Rigamonti	Carlo Rigamonti
							–						

Table 2. *Continued.* List of 69 tracks identified by the Stardust@home project. The columns are: stack number; azimuth angle of the particle trajectory in degrees, measured counterclockwise from the midnight (sunward) direction; the detection efficiency ξ, and the number of searches for each of phases I through IV; the cumulative detection efficiency ξ, and the number of searches; the first Stardust@home duster to identify the track; the Stardust@home Red Team members who identified and promoted the track to the α-list.

ID	ϕ	N_I	ξ_I	N_{II}	ξ_{II}	N_{III}	ξ_{III}	N_{IV}	ξ_{IV}	N_{mtotal}	ξ_{mtotal}	Duster discoverer	Red Team promoter(s)
2715058V1	4	0	–	0	–	0	–	11	0.91	11	–	Ronald C. Spencer	Michael A. Capraro
6493751V1	100	0	–	0	–	0	–	6	0.17	6	–	Martin St-pierre	Michael A. Capraro
19284V1	350	0	–	0	–	3	0	6	0.67	9	–	Tom Yahnke Sr.	SSL
535699V1	310	0	–	0	–	1	0	9	0.56	10	–	Tom Yahnke Sr.	SSL
709134V1	347	179	0.01	0	–	7	0	6	0.67	192	0.03	Cereal Killer	SSL
2293539V1	101	0	–	0	–	0	–	11	0.55	11	–	Charles Tabor	SSL
3726006V1	38	158	0.11	0	–	0	–	8	0.75	166	0.14	Paul Walboom	SSL
4028216V1	0	184	0.01	0	–	9	0.11	5	1	198	0.04	Bruce Hull	SSL
6031444V1	0	0	–	23	0.09	6	0.5	0	–	29	–	Jeremy Beckett	SSL
7510686V1	339	0	–	0	–	0	–	7	0.57	7	–	Vuillemot Christophe	SSL
9751354V1	37	0	–	0	–	0	–	8	0.63	8	–	Antonella Gastaldi	SSL
9659008V1	158	0	–	0	–	0	–	8	0.63	8	–	Maurizio Mandarino	Tom Yahnke Sr.
5958593V1	25	181	0.01	0	–	4	0	5	0.6	190	0.02	Daniel Smith	SSL

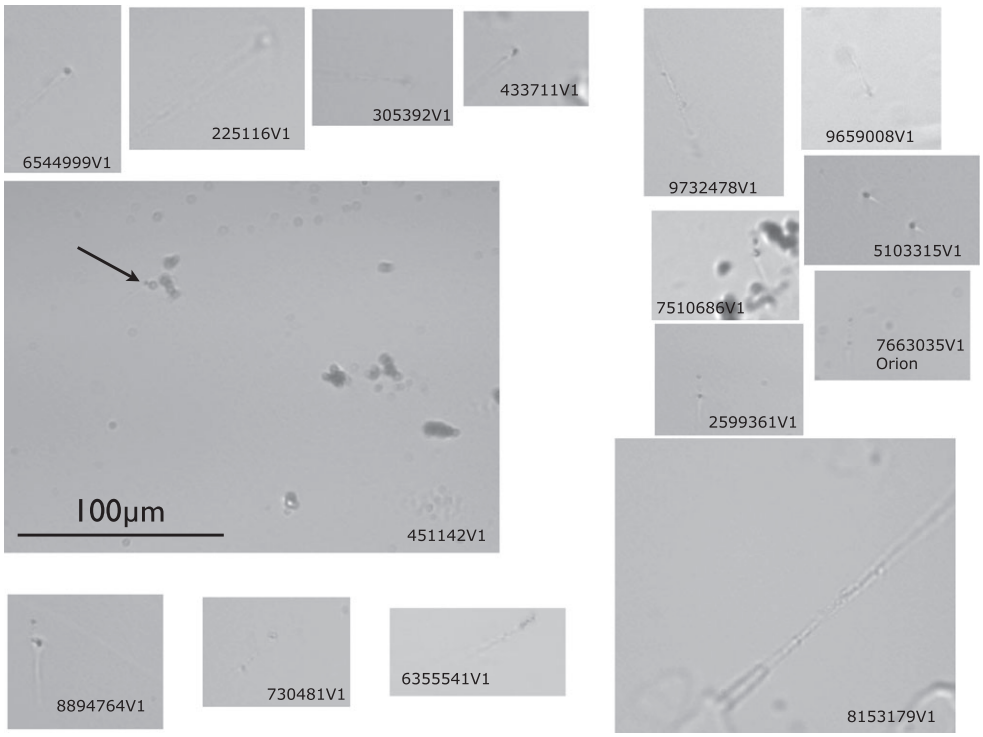

Fig. 5. Example images of tracks discovered by Stardust@home. The largest image, of track 451142V1, includes the entire field of view of the Virtual Microscope, and shows the scalebar. The other examples have been masked to show only the track, but all are shown at the same scale.

about the *x*- and *y*-axes, rotation by 180°); and stacks dubbed with images of tracks generated from submicron projectiles at the HDA (Postberg et al. 2014). The use of these calibrations resulted in dramatically higher ensemble-wide sensitivity in identification of real tracks (see, e.g., ξ_{IV} values in Table 2), although the statistics are smaller because of duster attrition over >5 years of operation. We conclude that detection efficiency improves dramatically when calibration images are presented that closely match the actual search targets.

A total of 69 unambiguous tracks were identified by Stardust@home. In Fig. 5, we show examples of the 69 tracks that were identified. Of these tracks, 21 were within 20° of the "midnight" direction (Westphal et al. 2014), which is consistent with an origin either in the interstellar dust stream, or with an origin as secondary ejecta from impacts on the Sample Return Capsule deck. This is discussed in more detail in the companion paper by Frank et al. (2013).

We conclude that a massively distributed, calibrated search, with amateur collaborators, is an effective approach to the challenging problem of identification of tracks of hypervelocity projectiles captured in aerogel. Because the actual tracks in the Stardust collector were morphologically strongly distinct from expectations, detection efficiency of actual tracks was lower than detection efficiency of calibrations presented in training, testing, and ongoing calibration. Presentation of actual tracks as calibrations resulted in very high detection efficiency for new tracks in Phase IV. A more precise measurement of overall detection efficiency for these small tracks will require the accumulation of better search statistics in Phase V and beyond.

Acknowledgments—We thank Sean Brennan and Giles Graham for thoughtful comments, and John Bradley for editorial handling. The ISPE consortium gratefully acknowledges the NASA Discovery Program for Stardust, the fourth NASA Discovery mission. AJW, ALB, ZG, RL, DZ, WM, and JVK were supported by NASA grant NNX09AC36G. We thank Steve Boggs for astrophysical soft X-ray spectra. RMS, HCG, and NDB were supported by NASA grant NNH11AQ61I. The Advanced Light Source is supported by the Director, Office of Science, Office of Basic Energy Sciences, of the U.S. Department of Energy under Contract No. DE-AC02-05CH11231. Use of the National Synchrotron Light Source, Brookhaven National Laboratory, was supported by the U.S. Department of Energy, Office of Science, Office of Basic

Energy Sciences, under Contract No. DE-AC02-98CH10886.

Editorial Handling—Dr. John Bradley

REFERENCES

Butterworth A. L., Westphal A. J., Tyliszczak T., Gainsforth Z., Stodolna J., Frank D., Allen C., Anderson D., Ansari A., Bajt S., Bastien R. S., Bassim N., Bechtel H. A., Borg J., Brenker F. E., Bridges J., Brownlee D. E., Burchell M., Burghammer M., Changela H., Cloetens P., Davis A. M., Doll R., Floss C., Flynn G., Grün E., Heck P. R., Hillier J. K., Hoppe P., Hudson B., Huth J., Hvide B., Kearsley A., King A. J., Lai B., Leitner J., Lemelle L., Leroux H., Leonard A., Lettieri R., Marchant W., Nittler L. R., Ogliore R., Ong W. J., Postberg F., Price M. C., Sandford S. A., Sans Tresseras J., Schmitz S., Schoonjans T., Silversmit G., Simionovici A., Solé V. A., Srama R., Stephan T., Sterken V., Stroud R. M., Sutton S., Trieloff M., Tsou P., Tsuchiyama A., Vekemans B., Vincze L., Korff J. V., Wordsworth N., Zevin D., Zolensky M. E., and >30000 Stardust@home dusters. 2014. Stardust Interstellar Preliminary Examination IV: Scanning transmission X-ray microscopy analyses of impact features in the Stardust Interstellar Dust Collector. *Meteoritics & Planetary Science*, doi:10.1111/maps.12220.

Frank D., Westphal A. J., Zolensky M. E., Gainsforth Z., Bastien R. S., Allen C., Anderson D., Ansari A., Bajt S., Bassim N., Bechtel H. A., Borg J., Brenker F. E., Bridges J., Brownlee D. E., Burchell M., Burghammer M., Butterworth A. L., Changela H., Cloetens P., Davis A. M., Doll R., Floss C., Flynn G., Grün E., Heck P. R., Hillier J. K., Hoppe P., Hudson B., Huth J., Hvide B., Kearsley A., King A. J., Lai B., Leitner J., Lemelle L., Leroux H., Leonard A., Lettieri R., Marchant W., Nittler L. R., Ogliore R., Ong W. J., Postberg F., Price M. C., Sandford S. A., Tresseras J. S., Schmitz S., Schoonjans T., Silversmit G., Simionovici A., Solé V. A., Srama R., Stephan T., Sterken V., Stodolna J., Stroud R. M., Sutton S., Trieloff M., Tsou P., Tsuchiyama A., Tyliszczak T., Vekemans B., Vincze L., Korff J. V., Wordsworth N., Zevin D., and >30000 Stardust@home dusters. 2013. Curating the Stardust interstellar dust collector: Picokeystones, the Stardust Interstellar Preliminary Examination (ISPE), and beyond. *Meteoritics & Planetary Science*, doi:10.1111/maps.12147.

Landgraf M., Müller M., and Grün E. 1999. Prediction of the in-situ dust measurements of the stardust mission to comet 81P/Wild 2. *Planetary and Space Science* 47:363.

McCray P. 2008. *Keep watching the skies! The story of Operation Moonwatch and the dawn of the space age*. Princeton, New Jersey: Princeton University Press.

Postberg F., Hillier J. K., Armes S. P., Bugiel S., Butterworth A. L., Dupin D., Fielding L. A., Fujii S., Gainsforth Z., Grün E., Li Y. W., Srama R., Sterken V., Stodolna J., Trieloff M., Westphal A. J., Allen C., Anderson D., Ansari A., Bajt S., Bastien R. S., Bassim N., Bechtel H. A., Borg J., Brenker F. E., Bridges J., Brownlee D. E., Burchell M., Burghammer M., Changela H., Cloetens P., Davis A. M., Doll R., Floss C., Flynn G., Frank D., Heck P. R., Hoppe P., Hudson B., Huth J., Hvide B., Kearsley A., King A. J., Lai B., Leitner J., Lemelle L., Leroux H., Leonard A., Lettieri R., Marchant W., Nittler L. R., Ogliore R., Ong W. J., Price M. C., Sandford S. A., Tresseras J. S., Schmitz S., Schoonjans T., Silversmit G., Simionovici A., Solé V. A., Stephan T., Stroud R. M., Sutton S., Tsou P., Tsuchiyama A., Tyliszczak T., Vekemans B., Vincze L., Korff J. V., Wordsworth N., Zevin D., Zolensky M. E., and >30000 Stardust@home dusters. 2014. High-speed interstellar dust analogue capture in Stardust fligh-spare aerogel. *Meteoritics & Planetary Science*, doi:10.1111/maps.12173.

Sterken V., Westphal A. J., Altobelli N., Grün E., Postberg F., Srama R., Allen C., Anderson D., Ansari A., Bajt S., Bastien R. S., Bassim N., Bechtel H. A., Borg J., Brenker F. E., Bridges J., Brownlee D. E., Burchell M., Burghammer M., Butterworth A. L., Changela H., Cloetens P., Davis A. M., Doll R., Floss C., Flynn G., Frank D., Gainsforth Z., Heck P. R., Hillier J. K., Hoppe P., Hudson B., Huth J., Hvide B., Kearsley A., King A. J., Lai B., Leitner J., Lemelle L., Leroux H., Leonard A., Lettieri R., Marchant W., Nittler L. R., Ogliore R., Ong W. J., Price M. C., Sandford S. A., Tresseras J. S., Schmitz S., Schoonjans T., Silversmit G., Simionovici A., Solé V. A., Stephan T., Sterken V., Stodolna J., Stroud R. M., Sutton S., Trieloff M., Tsou P., Tsuchiyama A., Tyliszczak T., Vekemans B., Vincze L., Korff J. V., Wordsworth N., Zevin D., Zolensky M. E., and >30000 Stardust@home dusters. 2014. Stardust Interstellar Preliminary Examination X: Impact speeds and directions of interstellar grains on the Stardust dust collector. *Meteoritics & Planetary Science*, doi:10.1111/maps.12219.

Tsou P., Brownlee D. E., Sandford S. A., Hörz F., and Zolensky M. E. 2003. Wild 2 and interstellar sample collection and Earth return. *Journal of Geophysical Research* 108:8113.

Westphal A. J., Altobelli N., Grün E., Postberg F., Srama R., Allen C., Anderson D., Ansari A., Bajt S., Bastien R. S., Bassim N., Bechtel H. A., Borg J., Brenker F. E., Bridges J., Brownlee D. E., Burchell M., Burghammer M., Butterworth A. L., Changela H., Cloetens P., Davis A. M., Doll R., Floss C., Flynn G., Frank D., Gainsforth Z., Heck P. R., Hillier J. K., Hoppe P., Hudson B., Huth J., Hvide B., Kearsley A., King A. J., Lai B., Leitner J., Lemelle L., Leroux H., Leonard A., Lettieri R., Marchant W., Nittler L. R., Ogliore R., Ong W. J., Price M. C., Sandford S. A., Tresseras J. S., Schmitz S., Schoonjans T., Silversmit G., Simionovici A., Solé V. A., Stephan T., Stodolna J., Stroud R. M., Sutton S., Trieloff M., Tsou P., Tsuchiyama A., Tyliszczak T., Vekemans B., Vincze L., Korff J. V., Wordsworth N., Zevin D., Zolensky M. E., and >30000 Stardust@home dusters. 2014. Final reports of the Stardust Interstellar Preliminary Examination. *Meteoritics & Planetary Science*, doi:10.1111/maps.12221.